Atmos. Chem. Phys. Discuss., 11, 15119–15155, 2011
www.atmos-chem-phys-discuss.net/11/15119/2011/
doi:10.5194/acpd-11-15119-2011

Atmospheric Chemistry and Physics Discussions

Quantification of the unknown HONO daytime source and its relation to NO_2

M. Sörgel[1,4], E. Regelin[2], H. Bozem[2,*], J.-M. Diesch[3], F. Drewnick[3], H. Fischer[2], H. Harder[2], A. Held[4], Z. Hosaynali-Beygi[2], M. Martinez[2], and C. Zetzsch[1,5]

[1]University of Bayreuth, Atmospheric Chemistry Research Laboratory, Bayreuth, Germany
[2]Max Planck Institute for Chemistry, Atmospheric Chemistry Department, P.O. Box 3060, 55020 Mainz, Germany
[3]Max Planck Institute for Chemistry, Particle Chemistry Department, P.O. Box 3060, 55020 Mainz, Germany
[4]University of Bayreuth, Junior Professorship in Atmospheric Chemistry, Bayreuth, Germany
[5]Fraunhofer Institute for Toxicology and Experimental Medicine, Hannover, Germany
[*]now at: University Mainz, Institute for Atmospheric Physics, Mainz, Germany

Received: 1 April 2011 – Accepted: 10 May 2011 – Published: 18 May 2011

Correspondence to: M. Sörgel (matthias.soergel@uni-bayreuth.de)

Published by Copernicus Publications on behalf of the European Geosciences Union.

Abstract

During the DOMINO (**Di**el **O**xidant **M**echanism **I**n relation to **N**itrogen **O**xides) campaign in southwest Spain we measured simultaneously all quantities necessary to calculate a photostationary state for HONO in the gas phase. These quantities comprise the concentrations of OH, NO, and HONO and the photolysis frequency of NO_2, $j(NO_2)$ as a proxy for j(HONO). This allowed us to calculate values of the unknown HONO daytime source. This unknown HONO source, normalized by NO_2 mixing ratios and expressed as a conversion frequency ($\%\,h^{-1}$), showed a clear dependence on $j(NO_2)$ with values up to $43\,\%\,h^{-1}$ at noon. We compared our unknown HONO source with values calculated from the measured field data for two recently proposed processes, the light-induced NO_2 conversion on soot surfaces and the reaction of electronically excited NO_2^* with water vapour, with the result that these two reactions normally contributed less than 10 % ($<1\%$ $NO_2 + \text{soot} + h\nu$; and $<10\,\%$ $NO_2^* + H_2O$) to our unknown HONO daytime source. OH production from HONO photolysis was found to be larger (by 20 %) than the "classical" OH formation from ozone photolysis ($O(^1D)$) integrated over the day.

1 Introduction

Nitrous acid (HONO) is an important OH radical precursor which serves as the "detergent" of the atmosphere due to its oxidizing power. Besides its importance for the atmospheric oxidation potential, HONO is part of acid and nutrient deposition to the biosphere. Moreover, growing concern exists about possible health effects due to the formation of nitrosamines (Hanst et al., 1977; Pitts et al., 1978) where HONO acts as the nitrosating agent, especially in indoor environments after wall reactions of HONO with nicotine (Sleiman et al., 2010). Despite three decades of research since the first unequivocal detection of HONO in the atmosphere (Perner and Platt, 1979), HONO formation processes in the atmosphere are still under discussion, especially during

Title Page
Abstract Introduction
Conclusions References
Tables Figures
◀| |▶
◀ ▶
Back Close
Full Screen / Esc
Printer-friendly Version
Interactive Discussion

daytime where large discrepancies were found between mixing ratios calculated from known gas phase chemistry and measured daytime mixing ratios (Kleffmann et al., 2005). In the absence of light, the most favoured formation reaction is the heterogeneous disproportionation of nitrogen dioxide (NO_2):

$$2NO_2 + H_2O \rightarrow HONO + HNO_3 \qquad (R1)$$

This reaction has been extensively studied on different materials like fluorinated polymers and different types of glass as reviewed by Lammel and Cape (1996), but also on building materials like concrete (Trick, 2004). It was found to be first order in NO_2 and water vapour (Sakamaki et al., 1983; Svennson et al., 1987; Pitts et al., 1984; Jenkin et al., 1988). A mechanism involving the formation of the NO_2 dimer (N_2O_4) in the gas phase was proposed (Finlayson-Pitts et al., 2003), but is not important in the real atmosphere (Kleffmann et al., 1998; Gustafsson et al., 2008). Recently, evidence for a mechanism involving reaction between adsorbed NO_2 and H (NO_2 (ads) + H(ads) → HONO (ads)) present on the surface following the dissociation of chemisorbed H_2O was found in a study on mineral dust particles with isotopically labelled water (Gustafsson et al., 2008), but the results are probably not transferable from laboratory to field conditions (Finlayson-Pitts, 2009). In the absence of light, HONO formation from NO_2 on soot deactivates quite rapidly and thus was concluded to be less important for atmospheric HONO formation except for freshly emitted soot (Kleffmann et al., 1999; Arens et al., 2001; Aubin and Abbatt, 2007). The mechanism was summarized as the Reaction (R2) of reducing organic compounds $\{C\text{-}H\}_{red}$ with NO_2 (Gutzwiller et al., 2002a). A reaction similar to Reaction (R2) was postulated for the aqueous phase (Gutzwiller et al., 2002b; Ammann et al., 2005), but only proceeds at a relevant rate at high pH levels, since it is based on the well-known charge transfer reaction of phenolate with NO_2.

$$NO_2 + \{C-H\}_{red} \rightarrow HONO + \{C\}_{ox} \qquad (R2)$$

$$NO + NO_2 + H_2O \rightarrow 2HONO \qquad (R3)$$

$$HNO_3(ads) + NO(g) \rightarrow HONO + NO_2 \tag{R4}$$

The Reactions (R3) (via the intermediate N_2O_3) and (R4) proposed from field measurements (Calvert et al., 1994; Andres-Hernandez et al., 1996; Saliba et al., 2001) could neither explain laboratory results under low NO_x conditions (Svensson et al., 1987; Jenkin et al., 1988; Kleffmann et al., 1998, 2004) nor field experiments with low NO mixing ratios (Harrison and Kitto, 1994; Alicke et al., 2003; this study).

During daytime the dominant sink for HONO is photolysis according to Reaction (R5), which forms OH.

$$HONO + h\nu \rightarrow NO + OH \tag{R5}$$

An additional sink is the reaction of HONO with OH (Reaction R6).

$$HONO + OH \rightarrow NO_2 + H_2O \tag{R6}$$

The Back Reaction (R7) regenerates HONO.

$$NO + OH + M \rightarrow HONO + M \tag{R7}$$

At high insolation, Reactions (R5–R7) are supposed to be in a photostationary state (PSS) (Cox, 1974; Kleffmann et al., 2005). Only few studies (Kleffmann et al., 2005; Acker et al., 2006) measured all quantities necessary to calculate the photostationary state (zero OH cycle), some with j(HONO) calculated from UV measurements (Ren et al., 2003, 2006). In all these studies measured HONO values exceeded the HONO values calculated from PSS. The "dark" heterogeneous formation (via Reactions R1/R2) was too slow (20–60 times) to explain this discrepancy (Kleffmann et al., 2003, 2005). This stimulated laboratory studies about a light-induced conversion of NO_2 to HONO or other photolytic sources of HONO as recently summarized by Kleffmann (2007).

There are a variety of proposed sources dealing with light-induced NO_2 reduction including NO_2 reduction on irradiated mineral surfaces like TiO_2 (Gustafsson et al., 2006; Ndour et al., 2008). Many studies focussed on the reduction of NO_2 involving organic photosensitizers (George et al., 2005) like hydrocarbons on soot (Monge et al., 2010) or humic acids (Stemmler et al., 2006; Stemmler et al., 2007). As already proposed from smog chamber experiments (Killus and Whitten, 1990), photolysis of deposited HNO_3/nitrate on surfaces was suggested as a daytime HONO source for rural environments by Zhou et al. (2002a), Zhou et al. (2002b) and Zhou et al. (2003) from field studies with low NO_x conditions. This mechanism is still controversial since the photolysis of HNO_3 was not found to be a photolytic source of HONO in chamber experiments (Rohrer et al., 2005). Quantum yields for HNO_3/nitrate photolysis are too low in the gas phase and in solution (Kleffmann, 2007), but this process can be enhanced at surfaces (Finlayson-Pitts, 2009) or via organic photosensitizers as speculated by Kleffmann (2007). Recent studies indeed proved the enhanced light absorption of surface adsorbed HNO_3 compared to the gas phase (Zhu et al., 2008, 2010).

A direct HONO source is the photolysis of nitrophenols (Bejan et al., 2006) depending on pollution levels which govern the formation of nitrophenols.

$$NO_2^* + H_2O \rightarrow HONO + OH \tag{R8}$$

The contribution of the reaction of electronically excited NO_2* with water vapour (Reaction R8) to the oxidation capacity of the troposphere was investigated in recent modelling studies (Wennberg and Dabdub, 2008; Sarwar et al., 2009; Ensberg et al., 2010). These studies focussed on ozone formation and concluded that there is an impact on oxidant formation for high NO_x emissions when using the rate constant of Li et al. (2008) for reactive quenching of NO_2*. Even with low NO_x emissions the influence is still noticeable, whereas using the rate constant of Crowley and Carl (1997) the impact is negligible. The portion of the reactive quenching of NO_2* by H_2O (and thus the rate constant of Reaction (R8), k_8) is still under discussion (Carr et al., 2009; Li et al., 2009; Fang et al., 2010; Blitz, 2010). In their laboratory study, Crowley and Carl (1997) did not observe any OH production via Reaction (R8) and thus derived an upper limit for the reactive quenching of NO_2* by H_2O of $k_8 = 1.2 \times 10^{-14}$ cm^3 molecules^{-1} s^{-1}. A recent study by Carr et al. (2009) confirmed these findings. In contrast to these studies which used unfocussed laser beams, Li et al. (2008) observed OH production and report a one order of magnitude higher value for $k_8 = 1.7 \times 10^{-13}\,\mathrm{cm^3\,molecules^{-1}\,s^{-1}}$.

In this study we quantify the gas phase photostationary state for HONO from measured values in Spain, calculate the values of the unknown HONO daytime source, and compare the latter with HONO formation from Reaction (R8) and the light-induced NO_2 conversion on soot (Monge et al., 2010).

2 Experimental

The **D**iel **O**xidant **M**echanism **I**n relation to **N**itrogen **O**xides (DOMINO) campaign took place at the "Atmospheric Sounding Station – El Arenosillo", a platform of the Atmospheric Research and Instrumentation Branch of the Spanish National Institute for Aerospace Technology (INTA) dedicated to atmospheric measurements in the southwest of Spain (37°05′48.03″ N, 6°44′07.47″ W). The measurement site was about 300 m inland from the coast of the Atlantic Ocean in a large area of uniform pine (*Pinus pinea* L.) forest with sandy soil. Only sparse buildings and streets were located around the site. About 15 km to the northwest is the industrial area of Huelva, with refineries and other heavy industry. The metropolitan area of Seville is about 70 km to the east-north-east. The campaign took place from mid November to mid December 2008.

Measurements of HONO were conducted at a height of 10 m above ground (∼4 m above canopy) on a scaffold and at 1 m above ground, by commercial LOPAP instruments (**LO**ng **P**ath **A**bsorption **P**hotometer, QUMA Elektronik & Analytik, Wuppertal, Germany). The LOPAP is based on a wet chemical technique, with fast sampling of HONO as nitrite in a stripping coil and subsequent detection as an azo dye using long path absorption in 2.4 m long Teflon AF tubing. A detailed description of the instrument has been given by Heland et al. (2001) and Kleffmann et al. (2002). The instruments were placed outside directly on the scaffolds in ventilated aluminium boxes without temperature control. The temperature of the stripping coils was kept constant at 20 °C by thermostats to assure constant sampling conditions.

The instrument used to measure NO_x was a high resolution and high sensitivity chemiluminescence detector (ECO-Physics CLD 790 SR, ECO-Physics, Dürnten, Switzerland) which carries out simultaneous in situ measurements of NO and NO_2. NO is measured directly, however, NO_2 is measured indirectly after conversion to NO using a blue light converter which is a solid state photolytic converter (Droplet Measurement Technologies, Boulder, CO, USA). A detailed description of the instrument and calibration techniques has been given by Hosaynali-Beygi et al. (2011).

Air was sampled through a polytetrafluoroethylene (PTFE) inlet line which was mounted on top of a scaffold at the measurement site at a height of 10 m above the ground. From there an inlet line which consisted of 1/2″ PTFE tubing was installed to the container. The last meter of the inlet line consisted of 1/4″ PTFE tubing. The total uncertainty for the original 1 s data (at 2σ) based on the calculations of precision and accuracy is 6.04 ppt + 5 % of reading for NO and 8.29 ppt + 8 % of reading for NO_2 measurements.

OH was measured by Laser Induced Fluorescence (LIF) with the "HORUS" (**H**ydr**O**xyl **R**adical measurement **U**nit based on fluorescence **S**pectroscopy) instrument (Martinez et al., 2010). The detection system was placed next to the LOPAP on top of the scaffold (10 m).

NO_2 photolysis frequencies $j(NO_2)$ were measured by filter radiometers (Meteorologie consult, Königstein, Germany) on top of the scaffold. The HONO photolysis frequency (j(HONO)) was calculated by multiplying $j(NO_2)$ with a factor of 0.175 (Trebs et al., 2009).

Photolysis frequencies for $O(^1D)$ formation ($j(O(^1D))$) were calculated using the TUV model (Version 4.1, e.g. Madronich et al., 1998) taking the ozone column from the NASA webpage (http://jwocky.gsfc.nasa.gov/teacher/ozone_overhead.html) and then scaling the calculated $O(^1D)$ values with the same factor as $j(NO_2)$ to measured $j(NO_2)$.

Meteorological parameters like temperature, relative humidity (RH), atmospheric pressure, wind speed and wind direction were measured with a Vaisala WXT510

(Vaisala, Helsinki, Finnland) meteorological station on top of the MoLa (**Mo**bile **La**boratory) inlet system, which was at 10 m height 10 m southeast of the scaffold. For details see Diesch et al. (2011).

MoLa measured ozone by UV absorption with the "Airpointer" (Recordum, Mödling, Austria), water vapour mixing ratios by infrared absorption (LICOR 840, Li-COR, Lincol, USA) and black carbon with a Multi Angle Absorption Photometer (MAAP, Model 5012, Thermo Fischer Scientific, Whatman, USA).

3 Results and discussion

3.1 Meteorological and chemical conditions

Figure 1 gives an overview of meteorological and chemical measurements during the experiment in November/December 2008. In the beginning of the campaign there was a fair weather period with moderate (about $3\,\mathrm{m\,s^{-1}}$) north-easterly winds (from inland Seville region). On 24 November, the wind direction changed to northwest (along the coast from Huelva). From the 28 to 30 November, clean marine air with some plumes arrived at the site from the west. This was also the only period with rainfall, and HONO values were often around the detection limit (2 ppt). Ozone mixing ratios were about 30 ppb and showed a diurnal variation except for the clean air period with higher values (40 ppb) and no diurnal variation. A more detailed analysis of the ozone behaviour and the different wind sectors has been given by Diesch et al. (2011).

3.2 Calculating the photo stationary state

Regarding only the well-established gas phase formation (R7) and gas phase sink processes (Reactions R5 and R6) one can calculate the photostationary state (PSS) mixing ratio of HONO (Cox, 1974; Kleffmann et al., 2005),

$$[\mathrm{HONO_{PSS}}] = \frac{k_7[\mathrm{NO}][\mathrm{OH}]}{k_6[\mathrm{OH}] + j(\mathrm{HONO})} \tag{1}$$

$[\mathrm{HONO_{PSS}}]$ is the equilibrium concentration, [NO] and [OH] are the measured NO and OH concentrations, and $j(\mathrm{HONO})$ is the photolysis frequency of HONO. For k_7 two values are recommended which differ by 24 % (constantly over the temperature and pressure range of our study): from IUPAC (Atkinson et al., 2004) $k_{7,(298\,\mathrm{K})} = 9.8 \times 10^{-12}\,\mathrm{cm^3\,molecules^{-1}\,s^{-1}}$ and from JPL (Sander et al., 2006) $k_{7,(298\,\mathrm{K})} = 7.4 \times 10^{-12}\,\mathrm{cm^3\,molecules^{-1}\,s^{-1}}$. This calculated JPL value is consistent with the value ($k_{7,(\sim 298\,K)} = (7.4 \pm 1.3) \times 10^{-12}\,\mathrm{cm^3\,molecules^{-1}\,s^{-1}}$) measured directely at atmospheric pressure by Bohn and Zetzsch (1997). We therefore prefer this value and use it for our calculations of the PSS. A rate constant of $k_{6,298\,\mathrm{K}} = 6.0 \times 10^{-12}\,\mathrm{cm^3\,molecules^{-1}\,s^{-1}}$ was taken for Reaction (R6) from Atkinson et al. (2004). Rate constants for the Termolecular Reaction (R7) were calculated from the fall-of curves according to the schemes given by the respective reference (Atkinson et al., 2004; Sander et al., 2006).

NO (±5 %) and $\mathrm{NO_2}$ photolysis frequencies ($j(\mathrm{NO_2}) \pm 5\,\%$) were measured very accurately. Thus, uncertainties in the PSS mainly originate from OH (±18 % accuracy) measurements which are very difficult. This has some influence on HONO formation via Reaction (R7) but not much influence on the loss term, since HONO loss via Reaction (R7) was mostly less than 5 % of the total loss (Reactions R5 + R6) during the whole campaign. As OH measurements may possibly suffer from interferences, the $[\mathrm{HONO_{PSS}}]$ values are rather an upper limit. As a consequence the unknown HONO source discussed in Sect. 3.3 is rather a lower limit. There is also some uncertainty in the $j(\mathrm{HONO})$ values since the portions of the upwelling part of the radiation measured at the site were about 0.3–0.5 of the downwelling (direct + diffuse). This high albedo values were presumably caused by the white container roofs and the aluminium scaffold below the sensor (in the morning also contribution of direct sunlight from the rising sun). As the minimum HONO lifetime (inverse photolysis frequency) is about 15 min around noon, our measurements at the 10 m scaffold do not reflect the local situation but an integration over a "footprint area" (Schmid, 2002; Vesala et al., 2008). Therefore, we chose an albedo value for UV radiation of the surrounding pine forest of 0.05 (Cancillo et al., 2005) which is more representative. Additionally, we estimated the uncertainty for the conversion of $j(NO_2)$ values into j(HONO) to be 5 % by comparing different parameterizations (Kraus and Hofzumahaus, 1998; Trebs et al., 2009) . The relative error of the HONO measurements is 12 % (Sörgel et al., 2011).

Figure 2 summarizes the diurnal courses of HONO and NO_x for 7 cloud free days. On the 27th around noon, fair weather clouds were passing. These data points were rejected for further analysis to exclude effects from fluctuations in j(HONO). On 2 December, data was taken from a second LOPAP at 1 m height. Both instruments have been demonstrated to agree within 12 % under dry field conditions in side-by-side measurements (Sörgel et al., 2011). Assuming efficient vertical mixing during the day, HONO mixing ratios at 1 m and 10 m height can be expected to be similar (Sörgel et al., 2011). The portion of HONO formed by known reactions in the gas phase ([$HONO_{PSS}$], Fig. 2b) is not negligible. Only 15 % of the data is below 10 % of the measured HONO mixing ratios. On the other hand, the gas phase formation can explain only part of the measured HONO, as 96 % of the [$HONO_{PSS}$] values are lower than the measured values by a factor of 2 or more.

$HONO_{meas}$, $HONO_{PSS}$, NO and NO_2 have a similar diurnal cycle with the most pronounced feature being the maximum values around 09:00 UTC. This could be explained by local emissions which were trapped in the stable boundary layer before the breakup of the inversion in the morning. In the afternoon (15:00–16:00), this peak occurs less pronouncedly in NO and NO_2 but very clearly in the PSS values, as OH values are about twice ($\sim 3 \times 10^6$ molecules cm^{-3}) those at 09:00. From Figs. 2b and d one can infer that [$HONO_{PSS}$] is dependent on NO mixing ratios ($r^2 = 0.78$). Measured HONO mixing ratios (Fig. 2a) have a coefficient of determination $r^2 = 0.49$ with [NO_2] and $r^2 = 0.36$ with [NO].

Interestingly, the HONO/NO_x ratios are always higher than those reported for direct emissions (max. reported 0.8 %) (Pitts et al., 1984; Kirchstetter et al., 1996; Kurtenbach et al., 2001; Kleffmann et al., 2003). This can be explained by efficient (up to 43 % h^{-1}) light-induced conversion of NO_2 during daytime (Sect. 3.3, Figs. 4b and 5). Around noon the influence of direct emissions is probably the lowest, as NO_x values exhibit a minimum and low variability. Furthermore, HONO lifetime is only about 15 min, so at typical wind speeds of about 3 m s^{-1}, emissions have to occur within 3 km to reach the site within their lifetime. During this period HONO/NO_x ratios reach their daytime maximum with values around 4 % (Fig. 2e), implying efficient NO_x conversion.

To sum up known HONO formation pathways, the heterogeneous formation (R1/R2) which was measured during nighttime may be included as an additional source in the PSS (e.g. Alicke et al., 2002, 2003) with the assumption that Reactions (R1/R2) continue at daytime in the same manner as at night.

This assumption may not be true because even at night HONO formation (release) is not proceeding at the same rate all night. Studies about HONO fluxes (Harrison and Kitto, 1994; Harrison et al., 1996; Stutz et al., 2002, 2004) explained that measured HONO formation is a net process (pseudo steady state) of release and deposition (see also discussion in Vogel et al., 2003). If no deposition or advection occurs, HONO/NO_x will rise continuously until sunrise, as photolysis is absent. We found decreasing HONO/NO_x in the late night until sunrise which may point to domination of loss processes of HONO, e.g. deposition. Therefore, it is questionable if Reactions (R1)/(R2), i.e. heterogeneous formation, can simply be transferred to daytime conditions. As will be shown in Sect. 3.3 (Figs. 3 and 4), including this dark heterogeneous source as a daytime source in Eq. (3) to calculate the magnitude of the unknown daytime source P_{unknown} yields mainly negative values in the early morning. This points to a missing sink like deposition (or a smaller source or both). Therefore, we did not consider this heterogeneous source for the PSS calculations.

Generally, a stable boundary layer is formed at nighttime in which turbulence is suppressed, whereas during daytime a mixed layer develops which is much more turbulent (e.g. Stull, 1988). This has two opposing effects on Reactions (R1)/(R2) (especially if the ground surface is the dominant source).

1. During daytime turbulence is enhanced which means that NO_2 is efficiently transported to the reactive surface.
2. The surface to volume ratio (S/V) is lower during daytime, as the mixed volume increases (mixed layer), thus less reactive surface area per volume is available.

There is ample evidence from ground based field measurements (Harrison and Kitto, 1994; Stutz et al., 2002; Veitel, 2002; Kleffmann et al., 2003; Zhang et al., 2009; Sörgel et al., 2011), aircraft profiles (Zhang et al., 2009) and modelling (Vogel et al., 2003) that the ground surface is a major source of HONO. Hence, turbulent exchange has a significant impact on near surface HONO mixing ratios as already proposed by Febo et al. (1996). These authors found a good correlation of HONO with radon, which is exclusively emitted from the ground. Furthermore, profiles from recent aircraft measurements were closely related to atmospheric stability with higher HONO values close to the ground and steeper gradients during stable conditions (Zhang et al., 2009). Therefore, mixing ratios should also be controlled by the mixed volume which determines the surface to volume ratio (S/V). The conventional way to account for changes in S/V is the scaling of HONO or HONO production (P_{HONO}) by NO_2 or NO_x (e.g. Alicke et al., 2002, 2003). It is assumed that NO_x is also emitted close to the ground, and therefore is also sensitive to S/V. As local sources/sinks may disturb this ratio, Su et al. (2008a) proposed a combined scaling using also black carbon (BC) and carbon monoxide (CO). To our knowledge, only two recent studies (Yu et al., 2009; Sörgel et al., 2011) tried to address S/V (ground and aerosol) directly by using inversion layer heights from SODAR measurements to estimate mixed volumes. However, at night a stable boundary layer is formed were only intermittent turbulence provides some mixing (Stull, 1988). Therefore, a mixed volume cannot easily be defined.

Apart from that, NO_2 conversion frequencies measured in different environments around the world are all within a quite narrow range from 0.4 to 1.8 % h^{-1} as summarized by Su et al. (2008a) and Sörgel et al. (2011). Conversion frequencies of 0.9–2 % h^{-1} for individual nights and a mean value of 1.5 ± 0.6 % h^{-1} were derived for this study. In our study, this nighttime HONO formation occurs presumably by (R1)/(R2). Formation through Reactions (R3), (R4) and (R7), all involving NO, cannot be important since HONO typically increased from sunset (17:30 UTC) to midnight, when NO mixing ratios were mostly (93 %) below the detection limit (LOD) of 6 ppt. Only 87 of 1232 five-minute mean values were above the LOD with mean/median mixing ratios of 20/8 ppt, respectively.

3.3 Missing daytime source

As shown in Sect. 3.2 (Fig. 2) measured HONO values ($HONO_{meas}$) almost always exceed the $[HONO]_{PSS}$ values. Thus, an additional (unknown) HONO daytime source exists. Equation (2), which is similar to that of Su et al. (2008b), sums up the processes influencing HONO mixing ratios.

$$\frac{\mathrm{dHONO}}{\mathrm{d}t} = \text{sources-sinks} == (P_{\mathrm{NO+OH}} + P_{\mathrm{emis}} + P_{\mathrm{het}} + P_{\mathrm{unknown}}) \\ -(L_{\mathrm{phot}} + L_{\mathrm{HONO+OH}} + L_{\mathrm{dep}}) + T_{\mathrm{v}} + T_{\mathrm{h}} \quad (2)$$

The source/production (P_x) terms consist of the gas phase formation (P_{NO+OH}, Reaction R7), the dark heterogeneous formation (P_{het}, via Reactions R1/R2) and direct emissions (P_{emis}). $P_{unknown}$ is the unknown HONO daytime source. The sink/loss processes (L_y) are photolysis (L_{phot}, Reaction R5), reaction of HONO with OH ($L_{HONO+OH}$, Reaction R6), and dry deposition (L_{dep}). Note that the terms for vertical (T_v) and horizontal advection (T_h) can mimic source or sink terms depending on the HONO mixing ratios of the advected air relative to that of the measurement site (and height). If HONO has a ground source (or near surface aerosol source), T_v mimics a sink term, as vertical mixing dilutes HONO formed near the ground (see also Sect. 3.2).

However, since we do not exactly know the sources of HONO and the vertical transport, we cannot quantify T_v. Su et al. (2008b) assumed T_v to be the same order as

L_{dep} and thus small compared to L_{phot}. L_{dep} can be parameterized by multiplying the measured HONO concentration with the dry deposition velocity and then scaling by the mixing height. Taking a deposition velocity of 2 cm s^{-1} (Harrison et al., 1996; Su et al., 2008b) and a mixing height of 1000 m, L_{dep} is in the order of a few ppt h^{-1} in our study which is indeed small (<3 % of L_{phot} 09:00–15:30 UTC for 7 clear days $N = 312$) compared to L_{phot}. As is discussed in more detail later, the relative contribution of L_{dep} might be higher in the morning and evening hours, as L_{phot} is smaller and a stable boundary layer is formed (mixed height $\ll$1000 m, or stable conditions). Overall, T_v and L_{dep} are small loss terms (compared to L_{phot}). If their contributions are larger than assumed (especially in the morning and evening), $P_{unknown}$ is underestimated during these periods.

P_{emis} cannot easily be determined, because its contribution varies with the source strength, the HONO lifetime, the horizontal wind speed and wind direction. Again, this contribution is assumed to be highest in the morning and in the evening (longer lifetimes = longer transport range). As there were no collocated emission sources, directly emitted HONO only contributed to the horizontal advection term (T_h).

Measured HONO/NO$_x$ ratios where always higher than reported for direct emissions (Sect. 3.2), thus no pure direct emissions were measured. Therefore, the contribution of directly emitted HONO to $P_{unknown}$ is uncertain, but P_{emis} can be assumed to be of minor importance around noon (Sect. 3.2).

Simplifying Eq. (2), we can derive the unknown HONO daytime source, $P_{unknown}$, from Eq. (3).

$$P_{unknown} = L_{HONO+OH} + L_{phot} + L_{dep} - P_{NO+OH} - P_{het} + \frac{\Delta HONO}{\Delta t} \tag{3}$$

P_{unknow} is not equal to OH production from HONO as for net OH formation a simple balancing of gas phase sources and sinks without further assumptions is applicable ($P_{OH} = L_{phot} - L_{HONO+OH} - P_{NO+OH}$). Mean diurnal contributions of the single terms and the values of $P_{unknown}$ are presented in Fig. 3. P_{NO+OH}, L_{phot}, $L_{HONO+OH}$ were calculated from measured values as already described for the PSS (Sect. 3.2). P_{het}

was parameterized from the nighttime measurements $P_{\text{het}}(t) = \overline{F_{\text{HONO,night}}}$ [NO$_2$] (Alicke et al., 2002) by assuming that the dark HONO formation ($F_{\text{HONO,night}}$) proceeds in the same manner as during the HONO mixing ratio increase at night (see Sect. 3.2 and discussion below). Using $F_{\text{HONO,night}} = 1.5\,\%\,\text{h}^{-1}$ (Sect. 3.2), P_{unknown} is negative (Figs. 3 and 4) in the early morning and evening indicating a missing sink, since more HONO is formed by the " known sources" than is destroyed via photolysis. A likely sink is non-negligible deposition of HONO, whose relative contribution might be higher in the morning and evening hours (mixed height $\ll$1000 m). The differential dHONO/dt was substituted by the difference ΔHONO/Δt, which is the mixing ratio difference from the centre of the interval (5 min) to the centre of the next interval (LOPAP has 5 min time resolution) and accounts for changes in mixing ratio levels. It became obvious that point to point changes in HONO (ΔHONO/Δt) were mostly smaller than the relative error of the instrument (±12 %), and so we could not account for these changes. Values above this threshold were mainly caused by sharp HONO peaks which were accompanied with peaks in NO and BC. These plumes passed the site mainly in the morning hours (see Figs. 2, 3 and 4) with maximum HONO values comparable to the nighttime maxima (Fig. 1). This indicates that especially in the morning, the advective term T_{h} does play a role and the arrival of plumes at the site mimics a source term (ΔHONO/$\Delta t > 0$), whereas their fading (ΔHONO/$\Delta t < 0$) mimics a sink (Figs. 3 and 4). Also, the contribution of ΔHONO/Δt to P_{unknown} depends on the integration time of the HONO signal. Comparing 5, 15, 30 and 60 min values, the highest contribution is associated with the 5 min values and the lowest with the 30 min values (60 min values are possibly already influenced by the diurnal cycle). Besides less influence from advection, the lower contribution of ΔHONO/Δt to the source and sink terms during the PRIDE-PRD-2004 experiment (Su et al., 2008b) compared to our study could at least partly be caused by the lower time resolution for HONO measurements in that study.

In Fig. 3 the diurnal course of the mean contributions of the single terms of Eq. (3) and the values for P_{unknown} are shown. The reaction between HONO and OH ($L_{\text{HONO+OH}}$) has a very small contribution to HONO loss (mostly less than 5 % of L_{phot}).

Dry deposition (L_{dep}) is also very small, but its relative contribution might be higher in the morning and evening. Around noon the main known HONO source is P_{NO+OH}. Due to low NO_2 levels around noon (see Fig. 2) P_{het} is also very low during that period. The noon period is clearly dominated by loss via L_{phot} (the overall dominant loss process) and formation by the unknown HONO source ($P_{unknown}$). P_{het} is higher in the morning and evening, respectively, provided that the parameterization (Sect. 2.3) is valid.

Figure 4a shows all calculated values of the unknown HONO source ($P_{unknown}$) in ppt h^{-1} ($= 7.37 \times 10^3$ molecules cm^{-3} s^{-1} at 1000 hPa and 273.15 K) versus $j(NO_2)$, as former studies (e.g. Vogel et al., 2003; Su et al., 2008b) proposed a correlation of this source to $j(NO_2)$. Values for $P_{unknown}$ range from about -700 to 1800 ppt h^{-1} (at noontime 10:00–14:00 UTC: 105 ± 39 ppt h^{-1} for 7 clear days $N = 195$) which is within the range of other rural and urban studies (Kleffmann, 2007; and Table 1). The filled red dots in Fig. 4 are points where $\Delta HONO/\Delta t$ values were larger than the respective relative errors of the HONO measurements, and thus included in Eq. (3).

As light-induced conversion of NO_2 is thought to be the most probable source of HONO daytime formation, we normalized the unknown source by the NO_2 mixing ratios to improve comparability to other environmental conditions (remote, urban, laboratory). This normalized $P_{unknown}$ presented in Fig. 4b has the same units (% h^{-1}) as the nightime conversion frequency ($F_{HONO,night}$) and can be referred to as a daytime conversion frequency assuming NO_2 is the direct precursor as indicated by recent studies of light-induced NO_2 conversion (e.g. Stemmler et al., 2006).

Figure 4b indicates that NO_2 levels indeed play an important role, as peak values of the daytime source, when scaled by NO_2 mixing ratios, fit into the “correlation scheme”. From Fig. 4b it seems that there is an upper limit for conversion of NO_2 to HONO depending on light intensity. Assuming that the dark heterogeneous conversion proceeds with the same rate during day as in the early night, its contribution to $P_{unknown}$ is very low during most of the day. This can be seen from a comparison with the diurnal cycle of the normalized $P_{unknown}$ in Fig. 5. While the maximum dark heterogeneous conversion rates are around 2 % h^{-1}, the normalized unknown source (presumably daytime

NO_2 conversion frequency) reaches median values of about 14 % h^{-1} around noontime, with maximum values up to 43 % h^{-1}. Around noon P_{unknown} is thus about 7 to 20 times faster than the parameterized nighttime conversion, which is in agreement with Kleffmann et al. (2003), but a factor of three lower than found by Kleffmann et al. (2005).

Table 1 presents a comparison of different field studies which quantified a HONO daytime source and the contribution of HONO to primary OH production. As the literature values were not normalized to NO_2, which would allow for better intercomparison, differences in the HONO daytime source seem to be mainly related to NO_x levels. Clearly, values for the rural/semi-rural sites range from 100 to about 600 ppt h^{-1} whereas values from the urban sites are about 2 to 3 times higher (1400–1600 ppt h^{-1}). Values for the contribution to primary OH formation vary a lot (6–56 %). In the rural/semirural environments, a substantial contribution (about 20–40 %), was found, with the exception of the study of Ren et al. (2010) with only 6 %. These authors explained that the difference might be caused by the low humidity and the low acid precipitation at Blodgett Forest causing low HONO values. Several field and modelling studies took place in urban environments (e.g. summarized by Volkamer et al., 2010). Contributions to OH formation from HONO vary a lot within these data (4–56 %), but not all studies measured daytime HONO values. Large differences even occur within the same city, e.g. for Mexico City with 12 % in the MCMA-2003 campaign (Volkamer et al., 2010) and 35 % in the MCMA-2006 campaign (Dusanter et al., 2009).

3.4 Potential contributions to the unknown HONO daytime source

In this section we investigate the contributions of two possible reaction pathways recently investigated in laboratory studies following a light-induced conversion of NO_2.

3.4.1 NO_2 conversion on irradiated soot

We calculated HONO production rates from the reaction of NO_2 on irradiated soot surfaces by extrapolating the reactive uptake coefficients (γ-values) derived in a laboratory study (Monge et al., 2010) to conditions we measured in the field. These γ-values were normalized to the Brunauer-Emmett-Teller surface (BET-surface) of the soot samples yielding a mass independent uptake (γ-BET). This γ-BET for NO_2 was found to increase with increasing irradiance and with decreasing NO_2 mixing ratios (Monge et al., 2010). Therefore, we used an extrapolation to lower NO_2 values ($\ll$16 ppb) provided by B. D'Anna (personal communication, 2010) leading to higher reactive NO_2 uptake in our study (median daytime $NO_2 = 0.9$ ppb). For simplicity, we took a value of $100\,\mathrm{m^2\,g^{-1}}$ as the BET surface for soot, which is between the values ($120–140\,\mathrm{m^2\,g^{-1}}$ from a propane flame) used by Monge et al. (2010) and a value of $97\,\mathrm{m^2\,g^{-1}}$ published for freshly emitted ($81\,\mathrm{m^2\,g^{-1}}$ for oxidized) soot (Daly and Horn, 2009). It can be regarded as an upper limit for soot from natural and anthropogenic combustion (Rockne et al., 2000; Fernandes et al., 2003). Black carbon (BC) measurements were taken as proxy soot values. As a further simplification, we used a constant upper limit integrated (300–420 nm) photon flux of 1.91×10^{16} photons $\mathrm{cm^{-2}\,s^{-1}}$ instead of varying it with the solar zenith angle. Therefore, the diurnal variation of the calculated values (Fig. 6) has to be viewed with caution. High values in the morning hours due to NO_2 and BC peaks are actually lower due to lower irradiance values in the morning, and thus lower reactivity. Following Monge et al. (2010), we assumed a HONO production of 60 % of the reactive NO_2 uptake. Although we used upper limits for all calculations, the resulting values for the HONO production by this source (Fig. 6) are mostly (85 %) below 1 % of P_{unknown}, with 98 % of the values below 5 %. Thus, for conditions encountered during our campaign (daytime BC_{median} ~300 $\mathrm{ng\,m^{-3}}$ and $NO_{2,\mathrm{median}} \sim 0.9$ ppb) this reaction has no noticeable influence on HONO daytime values.

3.4.2 Electronically excited NO_2 reacting with water vapour

In order to study the potential contribution of the controversially discussed reaction of electronically excited NO_2 with water vapour (Reaction R8), we calculated its contribution to HONO and OH formation using the expression for OH production (= HONO production) from Crowley and Carl (1997).

$$R_{OH} = j_{ex}(NO_2)[NO_2]/(1 + k_{air}[M]/k_8[H_2O]) \tag{4}$$

$j_{ex}(NO_2)$ is the frequency of electronic excitation of NO_2 beyond the dissociation threshold (>420 nm), and k_{air} the rate constant for non- reactive quenching with air. k_8 is the rate constant for the reactive quenching with H_2O, $k_{8,\text{Crowley}} = 1.2 \times 10^{-14}\,\text{cm}^3\,\text{molecules}^{-1}\,\text{s}^{-1}$ according to Crowley and Carl (1997) and $k_{8,\text{Li}} = 1.7 \times 10^{-13}\,\text{cm}^3\,\text{molecules}^{-1}\,\text{s}^{-1}$ according to Li et al. (2008). We estimated $j_{ex}(NO_2)$ from measured $j(NO_2)$ by multiplying with a factor of 3.5 (Crowley and Carl, 1997) which is consistent with solar zenith angles <70° (~60° around noontime).

Referring to $k_{8,\text{Li}}$ as an upper limit, HONO and OH production rates calculated via Eq. (4) are in the order of a few ppt h^{-1}, which is less than 10 % for 82 % of our data, with 58 % of our values <5 % of the unknown HONO source (P_{unknown}). Using $k_{8,\text{Crowley}}$, the values are one order of magnitude lower and thus negligible. These findings are in line with calculations from Crowley and Carl (1997) and with recent modelling studies (Wennberg and Dabdub, 2008; Sarwar et al., 2009; Ensberg et al., 2010) where this reaction was found to have a noticeable impact only at very high pollution levels, when using $k_{8,\text{Li}}$. As we do not expect the value for k_8 to be higher than reported by Li et al. (2008), we do not follow the approach of Wentzell et al. (2010) to explain the unknown HONO source by Reaction (R8) with varying k_8 alone.

3.5 Comparison of OH radical production from ozone and HONO photolysis

OH production rates from ozone photolysis were calculated from ozone, H_2O measurements and modelled $jO(^1D)$ values which were scaled by the ratio of measured and modelled $j(NO_2)$. OH production from $O(^1D)$ was calculated according to Crowley and

Carl (1997) using the rate constants for O(^{1}D) quenching by O_2, N_2 and O_3 and the reaction with H_2O taken from the IUPAC recommendations (Atkinson et al., 2004 and updated values from the IUPAC homepage, http://www.iupac-kinetic.ch.cam.ac.uk/). These values are in good agreement (~3 % higher) with the same calculations using the recommendations from Sander et al. (2006). The net OH production by HONO was calculated by balancing source and sink terms of OH by HONO in the gas phase (for k values see Sect. 3.2):

$$P_{OH} = j(\mathrm{HONO})[\mathrm{HONO}] - k_7[\mathrm{NO}][\mathrm{OH}] - k_6[\mathrm{HONO}][\mathrm{OH}] \quad (5)$$

Although HONO mixing ratios (mean: 30 ppt) are three orders of magnitude lower than O_3 mixing ratios (mean: 35 ppb) around noon and OH production rates by O(^{1}D) exceed those of HONO photolysis by about 50 % around noon (11:00–13:00), the integrated daily OH production is about 20 % lower than that of HONO. Figure 7 shows the higher contribution of HONO photolysis to the OH formation in the morning and evening hours due to longer wavelengths (up to ~400 nm) associated with HONO photolysis. A special feature of our measurement site are the very high HONO values between 08:00 and 11:00, which can be attributed to advection (see Sects. 3.2 and 3.3). This leads to high P_{OH} values from HONO photolysis during that period.

4 Conclusions

The unknown HONO daytime source derived from our measurements was normalized by NO_2 mixing ratios to improve comparability of HONO source strengths in different environmental and laboratory conditions. For the nighttime formation of HONO, we can exclude that NO plays an important role as NO was mostly below the detection limit of about 6 ppt. Inclusion of the parameterized nighttime HONO formation from NO_2 (1.5 % h^{-1} in this study) as an additional source into the calculations of the unknown HONO daytime source ($P_{unknown}$) yields mainly negative values in the early morning. This indicates the relevance of loss terms not taken into account (e.g. deposition) or overestimation of the dark heterogeneous formation in the morning and evening. Restricting the analysis only to cloud free days and the time around noon, when faster HONO photolysis leads to lifetimes around 15 min and other loss processes for HONO are small compared to loss by photolysis, establishment of a PSS can be assumed. The mean source strength of P_{unknown} under these conditions was about 100 ppt h^{-1} and thus in the lower range of values reported in the literature. Nevertheless P_{unknown} was the dominant HONO source during day. The normalized unknown HONO source (or NO_2 conversion frequency, if we assume that NO_2 is the precursor) varied from slightly negative values in the morning and evening to an upper limit correlated with $j(NO_2)$. High median daytime NO_2 conversion frequencies of ∼14 % h^{-1} were found around noon, in addition to the 1.5 % h^{-1} HONO formation rate observed during night.

Our results indicate light-induced HONO formation through conversion of NO_2, which is about an order of magnitude stronger than HONO formation during nighttime. We compared the HONO net source to values calculated for light-induced NO_2 uptake on soot (Monge et al., 2010) and the reaction of electronically excited NO_2^* with water vapour. The contribution of these reactions to HONO daytime values was mostly less than 10 % and cannot explain the HONO source strength derived in our study. Other processes like light-induced conversion of NO_2 on irradiated organic materials like humic acids (Stemmler et al., 2006) might be more important. Additional measurements including detailed speciation of organic aerosols and determination of humic acids on ground and canopy surfaces are needed to quantify their contribution. The unknown HONO daytime source is essential contribution to primary OH production, as photolysis of HONO exceeded the OH formation by ozone photolysis by 20 %.

Acknowledgements. The authors gratefully acknowledge financial support by the German Science foundation (DFG project ZE 792/4-1) and by the Max Planck Society. We are grateful to Ralph Dlugi and Thomas Foken for intensive and fruitful discussions. We thank Ivonne Trebs and Franz-Xaver Meixner from the Max Planck Institute for Chemistry for providing instruments and equipment, and the Spanish National Institute of Aerospace Technology (INTA) for hosting the campaign.

Title Page
Abstract Introduction
Conclusions References
Tables Figures
|◄ ►|
◄ ►
Back Close
Full Screen / Esc
Printer-friendly Version
Interactive Discussion

References

Acker, K., Möller, D., Wieprecht, W., Meixner, F. X., Bohn, B., Gilge, S., Plass-Dülmer, C., and Berresheim, H.: Strong daytime production of OH from HNO_2 at a rural mountain site, Geophys. Res. Lett., 33, L02809, doi:10.1029/2005GL024643, 2006.

Alicke, B., Platt, U., and Stutz, J.: Impact of nitrous acid photolysis on the total hydroxyl radical budget during the Limitation of Oxidant Production Pianura/Padana Produzione di Ozono study in Milan, J. Geophys. Res., 107, 8196, doi:10.1029/2000JD000075, 2002.

Alicke, B., Geyer, A., Hofzumahaus, A., Holland, F., Konrad, S., Pätz, H. W., Schäfer, J., Stutz, J., Volz-Thomas, A., and Platt, U.: OH formation by HONO photolysis during the BERLIOZ experiment, J. Geophys. Res., 108, 8247, doi:10.1029/2001JD000579, 2003.

Ammann, M., Rössler, E., Strekowski, R., and George, C.: Nitrogen dioxide multiphase chemistry: Uptake kinetics on aqueous solutions containing phenolic compounds, Phys. Chem. Chem. Phys., 7, 2513–2518, 2005.

Andres-Hernandez, M. D., Notholt, J., Hjorth, J., and Schrems, O.: A DOAS study on the origin of nitrous acid at urban and non-urban sites, Atmos. Environ., 30, 175–180, 1996.

Arens, F., Gutzwiller, L., Baltensperger, U., Gäggler, H. W., and Ammann, M.: Heterogeneous reaction of NO_2 on diesel soot particles, Environ. Sci. Technol., 35, 2191–2199, 2001.

Atkinson, R., Baulch, D. L., Cox, R. A., Crowley, J. N., Hampson, R. F., Hynes, R. G., Jenkin, M. E., Rossi, M. J., and Troe, J.: Evaluated kinetic and photochemical data for atmospheric chemistry: Volume I – gas phase reactions of O_x, HO_x, NO_x and SO_x species, Atmos. Chem. Phys., 4, 1461–1738, doi:10.5194/acp-4-1461-2004, 2004.

Aubin, D. G. and Abbatt, J. P. D.: Interaction of NO_2 with hydrocarbon soot: focus on HONO yield, surface modification, and mechanism, J. Phys. Chem. A, 111, 6263–6273, 2007.

Bejan, I., Abd el Aal, Y., Barnes, I., Benter, T., Bohn, B., Wiesen, P., and Kleffmann, J.: The photolysis of ortho-nitrophenols: a new gas phase source of HONO, Phys. Chem. Chem. Phys., 8, 2028–2035, doi:10.1039/b516590c, 2006.

Blitz, M. A.: Comment on "The conical intersection dominates the generation of tropospheric hydroxyl radicals from NO_2 and H_2O", J. Phys. Chem. A, 114, 8016, 2010.

Bohn, B. and Zetzsch, C.: Rate constants of HO_2 + NO covering atmospheric conditions. 1. HO_2 formed by OH + H_2O_2, J. Phys. Chem. A, 101, 1488–1493, 1997.

Calvert, J. G., Yarwood, G., and Dunker, A. M.: An evaluation of the mechanism of nitrous acid formation in the urban atmosphere, Res. Chem. Intermediat., 20, 463–502, 1994.

Cancillo, M. L., Serrano, A., Antón, M., García, J. A., Vilaplana, J. M., and de la Morena, B.: An improved outdoor calibration procedure for broadband ultraviolet radiometers, Photochem. Photobiol., 81, 860–865, 2005.

Carr, S., Heard, D. E., and Blitz, M. A.: Comment on "Atmospheric Hydroxyl Radical Production from Electronically Excited NO_2 and H_2O", Science, 324, p. 336, doi:10.1126/science.1166669, 2009.

Cox, R. A.: The photolysis of nitrous acid in the presence of carbon monoxide and sulphur dioxide, J. Photochem., 3, 291–304, 1974.

Crowley, J. N. and Carl, S. A.: OH formation in the photoexcitation of NO_2 beyond the dissociation threshold in the presence of water vapor, J. Phys. Chem. A, 101, 4178–4184, 1997.

Daly, H. M. and Horn, A. B.: Heterogeneous chemistry of toluene, kerosene and diesel soots, Phys. Chem. Chem. Phys., 11, 1069–1076, 2009.

Diesch, J.-M., Drewnick, F., Zorn, S. R., von der Weiden-Reinmüller, S.-L., Martinez, M., and Borrmann, S.: Variability of aerosol, trace gas and meteorological characteristics depending on continental, urban and marine air mass origins in the Southwestern Mediterranean, Atmos. Chem. Phys. Discuss., in review, 2011.

Dusanter, S., Vimal, D., Stevens, P. S., Volkamer, R., Molina, L. T., Baker, A., Meinardi, S., Blake, D., Sheehy, P., Merten, A., Zhang, R., Zheng, J., Fortner, E. C., Junkermann, W., Dubey, M., Rahn, T., Eichinger, B., Lewandowski, P., Prueger, J., and Holder, H.: Measurements of OH and HO_2 concentrations during the MCMA-2006 field campaign – Part 2: Model comparison and radical budget, Atmos. Chem. Phys., 9, 6655–6675, doi:10.5194/acp-9-6655-2009, 2009.

Elshorbany, Y. F., Kurtenbach, R., Wiesen, P., Lissi, E., Rubio, M., Villena, G., Gramsch, E., Rickard, A. R., Pilling, M. J., and Kleffmann, J.: Oxidation capacity of the city air of Santiago, Chile, Atmos. Chem. Phys., 9, 2257–2273, doi:10.5194/acp-9-2257-2009, 2009.

Ensberg, J. J., Carreras-Sospedra, M., and Dabdub, D.: Impacts of electronically photo-excited NO_2 on air pollution in the South Coast Air Basin of California, Atmos. Chem. Phys., 10, 1171–1181, doi:10.5194/acp-10-1171-2010, 2010.

Fang, Q., Han, J., Jiang, J., Chen, X., and Fang, W.: The conical intersection dominates the generation of tropospheric hydroxyl radicals from NO_2 and H_2O, J. Phys. Chem. A, 114, 4601–4608, 2010.

Febo, A., Perrino, C., and Allegrini, I.: Measurement of nitrous acid in Milan, Italy, by DOAS and diffusion denuders, Atmos. Environ., 30, 3599–3609, 1996.

Fernandes, M. B., Skjemstad, J. O., Johnson, B. B., Wells, J. D., and Brooks, P.: Characterization of carbonaceous combustion residues. I. Morphological, elemental and spectroscopic features, Chemosphere, 51, 785–795, 2003.

Finlayson-Pitts, B. J.: Reactions at surfaces in the atmosphere: integration of experiments and theory as necessary (but not necessarily sufficient) for predicting the physical chemistry of aerosols, Phys. Chem. Chem. Phys., 11, 7760–7779, 2009.

Finlayson-Pitts, B. J., Wingen, L. M., Sumner, A. L., Syomin, D., and Ramazan, K. A.: The heterogeneous hydrolysis of NO_2 in laboratory systems and in outdoor and indoor atmospheres: An integrated mechanism, Phys. Chem. Chem. Phys., 5, 223–242, 2003.

George, C., Strekowski, R. S., Kleffmann, J., Stemmler, K., and Ammann, M.: Photoenhanced uptake of gaseous NO_2 on solid organic compounds: a photochemical source of HONO?, Faraday Discuss., 130, 195–210, 2005.

Gustafsson, R. J., Orlov, A., Griffiths, P. T., Cox, R. A., and Lambert, R. M.: Reduction of NO_2 to nitrous acid on illuminated titanium dioxide aerosol surfaces: implications for photocatalysis and atmospheric chemistry, Chem. Commun., 37, 3936–3938, 2006.

Gustafsson, R. J., Kyriakou, G., and Lambert, R. M.: The molecular mechanism of tropospheric nitrous acid production on mineral dust surfaces, ChemPhysChem, 9, 1390–1393, 2008.

Gutzwiller, L., Arens, F., Baltensberger, U., Gäggler, H. W., and Ammann, M.: Significance of semivolatile diesel exhaust organics for secondary HONO formation, Environ. Sci. Technol., 36, 677–682, 2002a.

Gutzwiller, L., George, C., Rössler, E., and Ammann, M.: Reaction kinetics of NO_2 with resorcinol and 2,7-naphthalenediol in the aqueous phase at different pH, J. Phys. Chem. A, 106, 12045–12050, 2002b.

Hanst, P. L., Spence, J. W., and Miller, M.: Atmospheric chemistry of n-nitroso dimethylamine, Environ. Sci. Technol., 11, 403–405, 1977.

Harrison, R. M. and Kitto, A.-M. N.: Evidence for a surface source of atmospheric nitrous acid, Atmos. Environ., 28, 1089–1094, 1994.

Hosaynali Beygi, Z., Fischer, H., Harder, H. D., Martinez, M., Sander, R., Williams, J., Brookes, D. M., Monks, P. S., and Lelieveld, J.: Oxidation photochemistry in the Southern Atlantic boundary layer: unexpected deviations of photochemical steady state, Atmos. Chem. Phys. Discuss., 11, 7045–7093, doi:10.5194/acpd-11-7045-2011, 2011.

IUPAC Subcommittee on Gas Kinetic Data Evaluation: http://www.iupac-kinetic.ch.cam.ac.uk/, last access: January 2011.

Jenkin, M. E., Cox, R. A., and Williams, D. J.: Laboratory studies of the kinetics of formation of nitrous acid from the thermal reaction of nitrogen dioxide and water vapour, Atmos. Environ., 22 487–498, 1988.

Killus, J. P. and Whitten, G. Z.: Background reactivity in smog chambers, Int. J. Chem. Kinet., 22, 547–575, 1990.

Kirchstetter, T. W., Harley, R. A., and Littlejohn, D.: Measurement of nitrous acid in motor vehicle exhaust, Environ. Sci. Technol., 30, 2843–2849, 1996.

Kleffmann, J.: Daytime sources of nitrous acid (HONO) in the atmospheric boundary layer, Chem. Phys. Chem., 8, 1137–1144, 2007.

Kleffmann, J., Becker, K. H., and Wiesen, P.: Heterogeneous NO_2 conversion processes on acid surfaces: possible atmospheric implications, Atmos. Environ., 32, 2721–2729, 1998.

Kleffmann, J., Becker, K. H., Lackhoff, M., and Wiesen, P.: Heterogeneous conversion of NO_2 on carbonaceous surfaces, Phys. Chem. Chem. Phys., 1, 5443–5450, 1999.

Kleffmann, J., Kurtenbach, R., Lörzer, J., Wiesen, P., Kalthoff, N., Vogel, B., and Vogel, H.: Measured and simulated vertical profiles of nitrous acid – Part I: Field measurements, Atmos. Environ., 37, 2949–2955, 2003.

Kleffmann, J., Benter, T., and Wiesen, P.: Heterogeneous reaction of nitric acid with nitric oxide on glass surfaces under simulated atmospheric conditions, J. Phys. Chem. A, 108, 5793–5799, 2004.

Kleffmann, J., Gavriloaiei, T., Hofzumahaus, A., Holland, F., Koppmann, R., Rupp, L., Schlosser, E., Siese, M., and Wahner, A.: Daytime formation of nitrous acid: A major source of OH radicals in a forest, Geophys. Res. Lett., 32, L05818, doi:10.1029/2005GL022524, 2005.

Kraus, A. and Hofzumahaus, A.: Field measurements of atmospheric photolysis frequencies for O_3, NO_2, HCHO, CH_3CHO, H_2O_2, and HONO by UV spectroradiometry, J. Atmos. Chem., 31, 161–180, 1998.

Kurtenbach, R., Becker, K. H., Gomes, J. A. G., Kleffmann, J., Lörzer, J. C., Spittler, M., Wiesen, P., Ackermann, R., Geyer, A., and Platt, U.: Investigations of emissions and heterogeneous formation of HONO in a road traffic tunnel, Atmos. Environ., 35, 3385–3394, 2001.

Lammel, G. and Cape, J. N.: Nitrous acid and nitrite in the atmosphere, Chem. Soc. Rev., 25, 361–369, 1996.

Li, S., Matthews, J., and Sinha, A.: Atmospheric hydroxyl radical production from electronically excited NO_2 and H_2O, Science, 319, 1657–1660, doi:10.1126/science.1151443, 2008.

Li, S., Matthews, J., and Sinha, A.: Response to comment on "Atmospheric hydroxyl radical production from electronically excited NO_2 and H_2O", Science, 324, p. 336c, 2009.

Madronich, S. and Flocke, S.: The role of solar radiation in atmospheric chemistry, in The Handbook of Environmental Chemistry/Reactions and Processes/Environmental Photochemistry Part I: BD 2/Part L, edited by: Boule, P., Springer-Verlag, Heidelberg, 373, 1–26, 1998.

Martinez, M., Harder, H., Kubistin, D., Rudolf, M., Bozem, H., Eerdekens, G., Fischer, H., Klüpfel, T., Gurk, C., Königstedt, R., Parchatka, U., Schiller, C. L., Stickler, A., Williams, J., and Lelieveld, J.: Hydroxyl radicals in the tropical troposphere over the Suriname rainforest: airborne measurements, Atmos. Chem. Phys., 10, 3759–3773, doi:10.5194/acp-10-3759-2010, 2010.

Monge, M. E., D'Anna, B., Mazri, L., Giroir-Fendler, A., Ammann, M., Donaldson, D. J., and George, C.: Light changes the atmospheric reactivity of soot, P. Natl. Acad. Sci. USA, 107, 6605–6609, 2010.

NASA.: Ozone over your house, http://jwocky.gsfc.nasa.gov/teacher/, last access: January 2011.

Ndour, M., D'Anna, B., George, C., Ka, O., Balkanski, Y., Kleffmann, J., Stemmler, K., and Ammann, M.: Photoenhanced uptake of NO_2 on mineral dust: Laboratory experiments and model simulations, Geophys. Res. Lett., 35, L05812, doi:10.1029/2007GL032006, 2008.

Perner, D. and Platt, U.: Detection of nitrous acid in the atmosphere by differential optical absorption, Geophys. Res. Lett., 6, 917–920, 1979.

Pitts Jr., J. N., Grosjean, D., Cauwenberghe, K. V., Schmid, J. P., and Fitz, D. R.: Photooxidation of aliphatic amines under simulated atmospheric conditions: formation of nitrosamines, nitramines, amides, and photochemical oxidant, Environ. Sci. Technol., 12, 946–953, 1978.

Pitts Jr., J. N., Biermann, H. W., Winer, A. M., and Tuazon, E. C.: Spectroscopic identification and measurement of gaseous nitrous acid in dilute auto exhaust, Atmos. Environ., 18, 847–854, 1984.

Ren, X., Harder, H., Martinez, M., Lesher, R. L., Oliger, A., Simpas, J. B., Brune, W. H., Schwab, J. J., Demerjian, K. L., He, Y., Zhou, X., and Gao, H.: OH and HO_2 chemistry in the urban atmosphere of New York City, Atmos. Environ., 37, 3639–3651, 2003.

Ren, X., Brune, W. H., Mao, J., Mitchell, M. J., Lesher, R. L., Simpas, J. B., Metcalf, A. R., Schwab, J. J., Cai, C., Li, Y., Demerjian, K. L., Felton, H. D., Boynton, G., Adams, A., Perry, J., He, Y., Zhou, X., and Hou, J.: Behavior of OH and HO_2 in the winter atmosphere in New York City, Atmos. Environ., 40, 252–263, 2006.

Ren, X., Gao, H., Zhou, X., Crounse, J. D., Wennberg, P. O., Browne, E. C., LaFranchi, B. W., Cohen, R. C., McKay, M., Goldstein, A. H., and Mao, J.: Measurement of atmospheric nitrous acid at Bodgett Forest during BEARPEX2007, Atmos. Chem. Phys., 10, 6283–6294, doi:10.5194/acp-10-6283-2010, 2010.

Rockne, K. J., Taghon, G. L., and Kosson, D. S.: Pore structure of soot deposits from several combustion sources, Chemosphere, 41, 1125–1135, 2000.

Rohrer, F., Bohn, B., Brauers, T., Brüning, D., Johnen, F.-J., Wahner, A., and Kleffmann, J.: Characterisation of the photolytic HONO-source in the atmosphere simulation chamber SAPHIR, Atmos. Chem. Phys., 5, 2189–2201, doi:10.5194/acp-5-2189-2005, 2005.

Sakamaki, F., Hatakeyama, S., and Akimoto, H.: Formation of nitrous acid and nitric oxide in the heterogeneous dark reaction of nitrogen dioxide and water vapour, Int. J. Chem. Kinet., 15, 1013–1029, 1983.

Saliba, N. A., Yang, H., and Finlayson-Pitts, B. J.: Reaction of gaseous nitric oxide with nitric acid on silica surfaces in the presence of water at room temperature, J. Phys. Chem. A, 105, 10339–10346, 2001.

Sander, S. P., Friedl, R. R., Golden, D. M., Kurylo, M. J., Moortgat, G. K., Keller-Rudek, H., Wine, P. H., Ravishankara, A. R., Kolb, C. E., Molina, M. J., Finlayson-Pitts, B. J., Huie, R. E., and Orkin, V. L.: Chemical kinetics and photochemical data for use in atmospheric studies evaluation number 15, Jet Propulsion Laboratory, Pasadena, 523, 2006.

Sarwar, G., Pinder, R. W., Appel, K. W., Mathur, R., and Carlton, A. G.: Examination of the impact of photoexcited NO_2 chemistry on regional air quality, Atmos. Environ., 43, 6383–6387, 2009.

Schmid, H. P.: Footprint modeling for vegetation atmosphere exchange studies: a review and perspective, Agr. Forest. Meteorol., 113, 159–183, 2002.

Sleiman, M., Gundel, L. A., Pankow, J. F., Jacob, P., Singer, B. C., and Destaillats, H.: Formation of carcinogens indoors by surface-mediated reactions of nicotine with nitrous acid, leading to potential thirdhand smoke hazards, P. Natl. Acad. Sci. USA, 107(15), 6576–6581, 2010.

Sörgel, M., Trebs, I., Serafimovich, A., Moravek, A., Held, A., and Zetzsch, C.: Simultaneous HONO measurements in and above a forest canopy: influence of turbulent exchange on mixing ratio differences, Atmos. Chem. Phys., 11, 841–855, doi:10.5194/acp-11-841-2011, 2011.

Stemmler, K., Ammann, M., Donders, C., Kleffmann, J., and George, C.: Photosensitized reduction of nitrogen dioxide on humic acid as a source of nitrous acid, Nature, 440, 195–198, 2006.

Stemmler, K., Ndour, M., Elshorbany, Y., Kleffmann, J., D'Anna, B., George, C., Bohn, B., and Ammann, M.: Light induced conversion of nitrogen dioxide into nitrous acid on submicron humic acid aerosol, Atmos. Chem. Phys., 7, 4237–4248, doi:10.5194/acp-7-4237-2007, 2007.

Stull, R. B.: An introduction to boundary layer meteorology, Atmospheric and Oceanographic Sciences Library, Kluwer Academic Publishers, Dordrecht, 670 pp., 1988.

Stutz, J., Alicke, B., and Neftel, A.: Nitrous acid formation in the urban atmosphere: Gradient measurements of NO_2 and HONO over grass in Milan, Italy, J. Geophys. Res., 107, 8192, doi:10.1029/2001JD000390, 2002.

Stutz, J., Alicke, B., Ackermann, R., Geyer, A., Wang, S., White, A. B., Williams, E. J., Spicer, C. W., and Fast, J. D.: Relative humidity dependence of HONO chemistry in urban areas, J. Geophys. Res., 109, D03307, doi:10.1029/2003JD004135, 2004.

Su, H., Cheng, Y. F., Cheng, P., Zhang, Y. H., Dong, S., Zeng, L. M., Wang, X., Slanina, J., Shao, M., and Wiedensohler, A.: Observation of nighttime nitrous acid (HONO) formation at a non-urban site during PRIDE-PRD2004 in China, Atmos. Environ., 42, 6219–6232, 2008a.

Su, H., Cheng, Y. F., Shao, M., Gao, D. F., Yu, Z. Y., Zeng, L. M., Slanina, J., Zhang, Y. H., and Wiedensohler, A.: Nitrous acid (HONO) and its daytime sources at a rural site during the 2004 PRIDE-PRD experiment in China, J. Geophys. Res., 113, D14312, doi:10.1029/2007JD009060, 2008b.

Svennson, R., Ljungstrom, E., and Lindqvist: Kinetics of the reaction between nitrogen dioxide and water vapour, Atmos. Environ., 21 1529–1539, 1987.

Trebs, I., Bohn, B., Ammann, C., Rummel, U., Blumthaler, M., Königstedt, R., Meixner, F. X., Fan, S., and Andreae, M. O.: Relationship between the NO_2 photolysis frequency and the solar global irradiance, Atmos. Meas. Tech., 2, 725–739, doi:10.5194/amt-2-725-2009, 2009.

Trick, S.: Formation of nitrous acid on urban surfaces - a physical-chemical perspective-, Ph.D. thesis, University Heidelberg, Germany, 290 pp., 2004.

Veitel, H.: Vertical profiles of NO_2 and HONO in the boundary layer, Ph.D. thesis, University, Heidelberg, Germany, 270 pp., 2002.

Vesala, T., Kljun, N., Rannik, Ü., Rinne, J., Sogachev, A., Markkanen, T., Sabelfeld, K., Foken, T., and Leclerc, M. Y.: Flux and concentration footprint modelling: State of the art, Environ. Pollut., 152, 653–666, 2008.

Vogel, B., Vogel, H., Kleffmann, J., and Kurtenbach, R.: Measured and simulated vertical profiles of nitrous acid – Part II. Model simulations and indications for a photolytic source, Atmos. Environ., 37, 2957–2966, 2003.

Volkamer, R., Sheehy, P., Molina, L. T., and Molina, M. J.: Oxidative capacity of the Mexico City atmosphere – Part 1: A radical source perspective, Atmos. Chem. Phys., 10, 6969–6991, doi:10.5194/acp-10-6969-2010, 2010.

Wennberg, P., O. and Dabdub, D.: Rethinking ozone production, Science, 319, 1624–1625, 2008.

Wentzell, J. J. B., Schiller, C. L., and Harris, G. W.: Measurements of HONO during BAQS-Met, Atmos. Chem. Phys., 10, 12285–12293, doi:10.5194/acp-10-12285-2010, 2010.

Yu, Y., Galle, B., Panday, A., Hodson, E., Prinn, R., and Wang, S.: Observations of high rates of NO_2-HONO conversion in the nocturnal atmospheric boundary layer in Kathmandu, Nepal, Atmos. Chem. Phys., 9, 6401–6415, doi:10.5194/acp-9-6401-2009, 2009.

Zhang, N., Zhou, X., Shepson, P. B., Gao, H., Alaghmand, M., and Stirm, B.: Aircraft measurement of HONO vertical profiles over a forested region, Geophys. Res. Lett., 36, L15820, doi:10.1029/2009GL038999, 2009.

Zhou, X., Civerolo, K., Dai, H., Huang, G., Schwab, J., and Demerjian, K.: Summertime nitrous acid chemistry in the atmospheric boundary layer at a rural site in New York State, J. Geophys. Res., 107(D21), 4590, doi:10.1029/2001JD001539, 2002a.

Zhou, X., He, Y., Huang, G., Thornberry, T. D., Carroll, M. A., and Bertman, S. B.: Photochemical production of nitrous acid on glass sample manifold surface, Geophys. Res. Lett., 29, 1681, doi:10.1029/2002GL015080, 2002b.

Zhou, X., Gao, H., He, Y., Huang, G., Bertman, S. B., Civerolo, K., and Schwab, J.: Nitric acid photolysis on surfaces in low-NOx environments: Significant atmospheric implications, Geophys. Res. Lett., 30(23), 2217, doi:10.1029/2003GL018620, 2003.

Zhu, C., Xiang, B., Zhu, L. and Cole, R.: Determination of absorption cross sections of surface-adsorbed HNO_3 in the 290–330 nm region by Brewster angle cavity ring-down spectroscopy, Chem. Phys. Lett., 458, 73–377, 2008.

Zhu, C., Xiang, B., Chu, L. T., and Zhu, L.: Photolysis of nitric acid in the gas phase, on aluminum surfaces, and on ice films, J. Phys. Chem. A, 114, 2561–2568, 2010.

Table 1. Intercomparison of values of the HONO daytime source from rural and urban sites, as well as the contribution of HONO photolysis to primary OH formation. * Conversion at 900 hPa because the station Hohenpeissenberg is located ∼1000 m a.s.l.; ** only $L_{\mathrm{Phot}} - P_{\mathrm{NO+OH}}$.

location/region	measured	PSS	daytime source ppt h^{-1}	primary OH production in %	reference
Hohenpeissenberg/ rural	HONO (denuder), OH (CIMS), j(HONO) (spectroroadiometer), NO (chemiluminiscence)	all quantities measured	* 2–4×10^6 molecules cm^{-3} s^{-1} => ∼ 300–650	42	Acker et al. (2006)
Jülich Forest (ECHO)/semi rural	HONO (LOPAP), OH (LIF), j(HONO) (spectroradiometer), NO (chemiluminescence)	all quantities measured	∼ 500	33 (around noon)	Kleffmann et al. (2005)
Pinnacle State Park/rural	HONO (HPLC-Scrub), NO (chemiluminescence), j(HONO) (Epply TUVR)	OH calculated, j(HONO) calc from UV measurements	∼ 220 (40 ppt h^{-1} NO+OH) => 180 net	24	Zhou et al. (2002)
New York PMTACS-NY 2001 Summer/ megacity	HONO (HPLC-Scrub), OH (LIF), NO (chemiluminescence) j(HONO) (UV-MFRSR)	j(HONO) calculated	** about 10^7 molecules cm^{-3} s^{-1} => ∼ 1400	56 (day and night average)	Ren et al. (2003)
PMTACS-NY 2004 Winter/megacity	HONO (HPLC-Scrub), OH (LIF), NO (chemiluminescence)	j(HONO) calculated	–	48 (day and night average)	Ren et al. (2006)
Santiago Chile/ urban	HONO (LOPAP), NO (chemiluminescence), j(HONO) (filterradiometer j(NO_2))	OH modelled	1700 mean	55	Elshorbany et al. (2009)
Blodgett Forest/ rural	HONO (LOPAP custom built), OH (LIF)	NO and j(HONO) calculated	(1590 d^{-1})	6 (day and night average)	Ren et al. (2010)
"El Arenosillo"/ rural	HONO (LOPAP), NO (chemiluminescence), OH (LIF), j(HONO) (filteradiometer j(NO_2))	all quantities measured	105 ± 39 noontime max ∼ 500 in plumes	20 % more than O(^{1}D)	This study

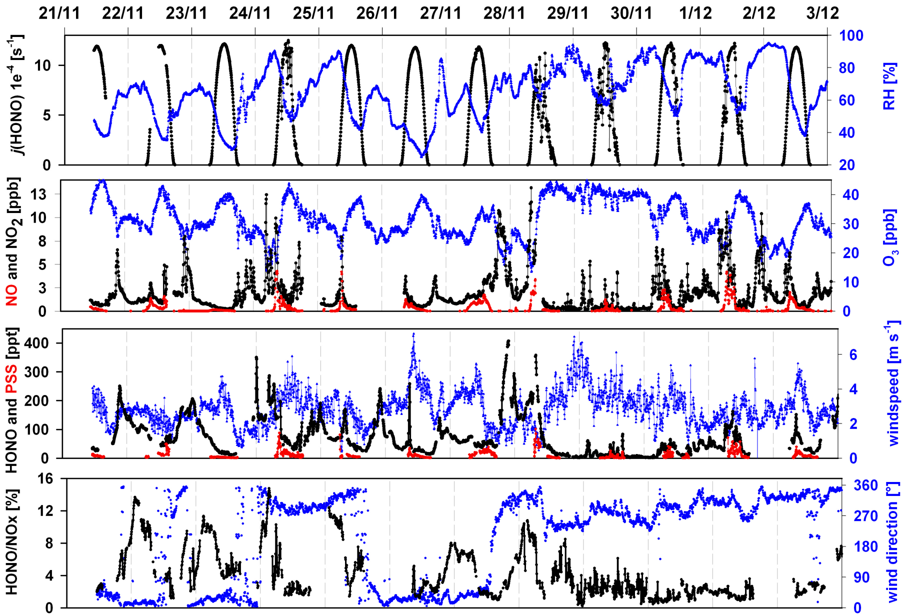

Fig. 1. Overview of meteorological (RH, wind speed and wind direction) and chemical quantities (O_3, NO, NO_2, HONO, $HONO_{PSS}$ (calculated), HONO/NO_x ratio and j(HONO)).

Title Page
Abstract
Introduction
Conclusions
References
Tables
Figures
◀|
|▶
◀
▶
Back
Close
Full Screen / Esc
Printer-friendly Version
Interactive Discussion

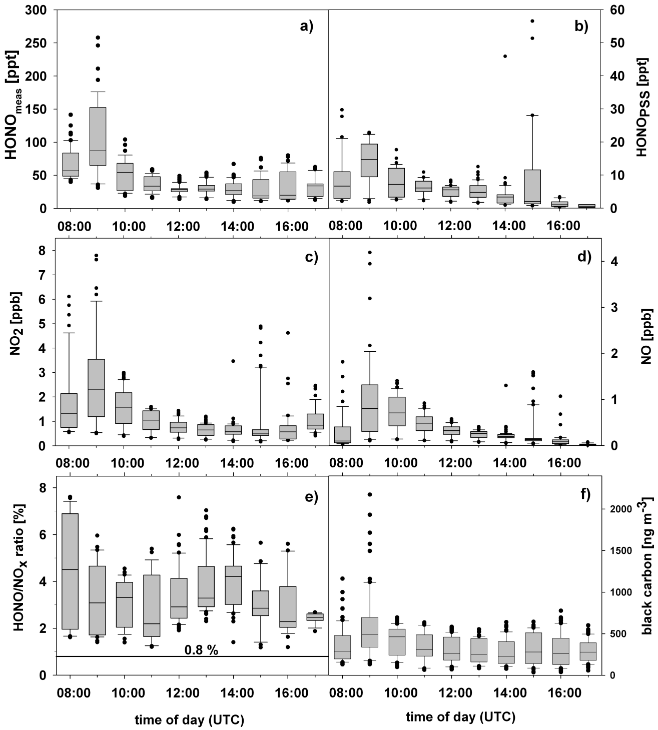

Fig. 2. Daytime cycles of **(a)** measured HONO mixing ratios, HONO$_{meas}$ **(b)** calculated HONO mixing according to Eq. (1), HONO$_{PSS}$ **(c)** NO$_2$ and **(d)** NO mixing ratios as well as **(e)** HONO/NO$_x$ ratios and black carbon concentration **(f)**. The boxes and whiskers represent a one hour time interval (centred in the middle) of five minute data (22–72 data points) of 7 cloud free days (21, 22, 23, 25, 26, 27 November and 2 December). The upper ends of the boxes represent the 75th percentile, the lower bounds the 25th percentile and the line within the boxes the median. The upper whisker marks the last point within the 90th percentile and the lower whisker that of the 10th percentile. Data points outside the 10th and 90th percentile are marked individually as dots.

Title Page
Abstract
Introduction
Conclusions
References
Tables
Figures
◀▮
▶▮
◀
▶
Back
Close
Full Screen / Esc
Printer-friendly Version
Interactive Discussion

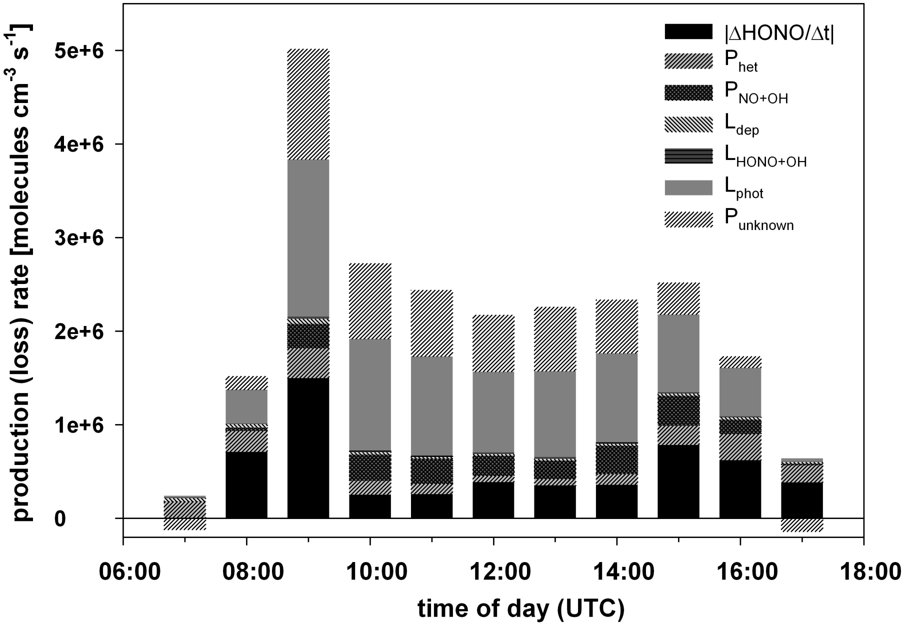

Fig. 3. Contributions of source and sink terms (hourly means 21 November to 5 December) as well as the unknown daytime HONO source P_{unknown} from Eq. (3).

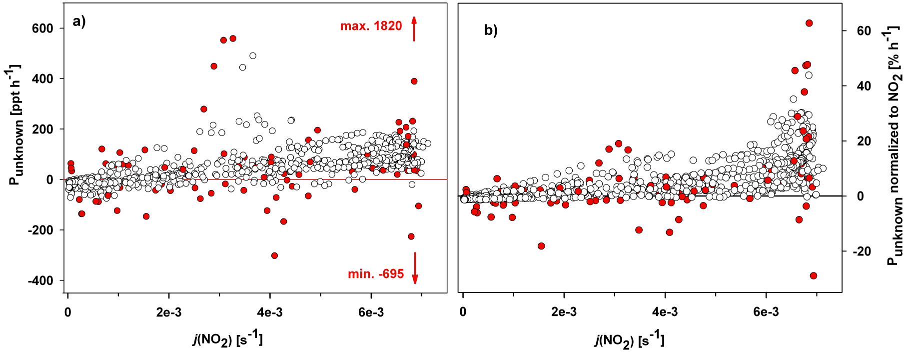

Fig. 4. **(a)** Unknown HONO daytime source (P_{unknown}) in ppt h^{-1} for all days versus $j(NO_2)$. **(b)** P_{unknown} normalized by NO_2 mixing ratios yielding a conversion frequency (% h^{-1}). Panel **(a)** contains only data points ($N = 753$) which could be normalized to NO_2. Points where ΔHONO/Δt was larger than the relative error of the LOPAP (±12 %) are marked as filled red points.

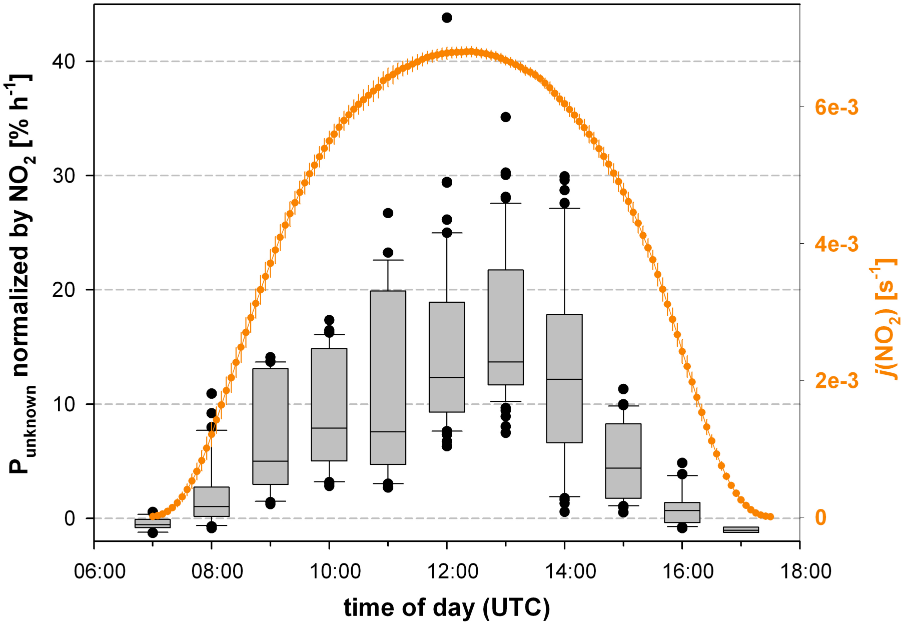

Fig. 5. Diurnal cycle (only daytime) of the unknown HONO source ($P_{unknown}$), normalized by NO_2 mixing ratios from 7 cloud-free days (same as Fig. 2). To reflect more stationary conditions, only values where $\Delta HONO/\Delta t$ was lower than the relative error of the LOPAP were included in this graph. The upper ends of the bars reflect the 75th percentiles, the lower bounds the 25th percentiles and the line in between the medians. The upper whiskers represents the 90th percentiles and the lower the 10th percentiles. The minimum number of data points per hour is 17 (07:00), the maximum is 59 (13:00), except for the values close to sunset (17:00) with only 8 data points. Orange dots and bars represent the mean and standard deviation of $j(NO_2)$ for these days, respectively.

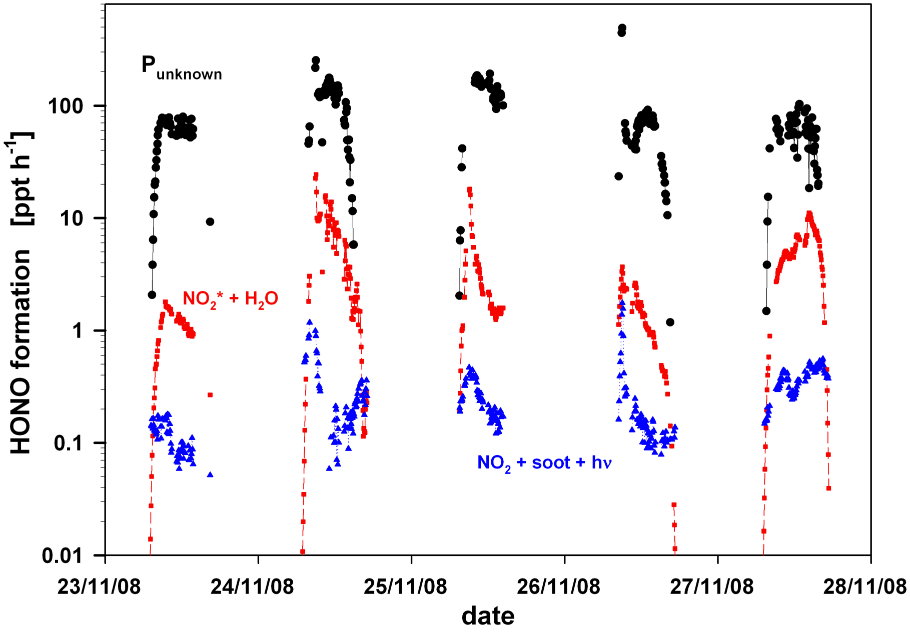

Fig. 6. Comparison of different HONO daytime source strengths (blue: NO_2 + soot + hν (Monge et al., 2010); red: NO_2^* + H_2O, Li et al., 2008) with the unknown HONO daytime source (black).

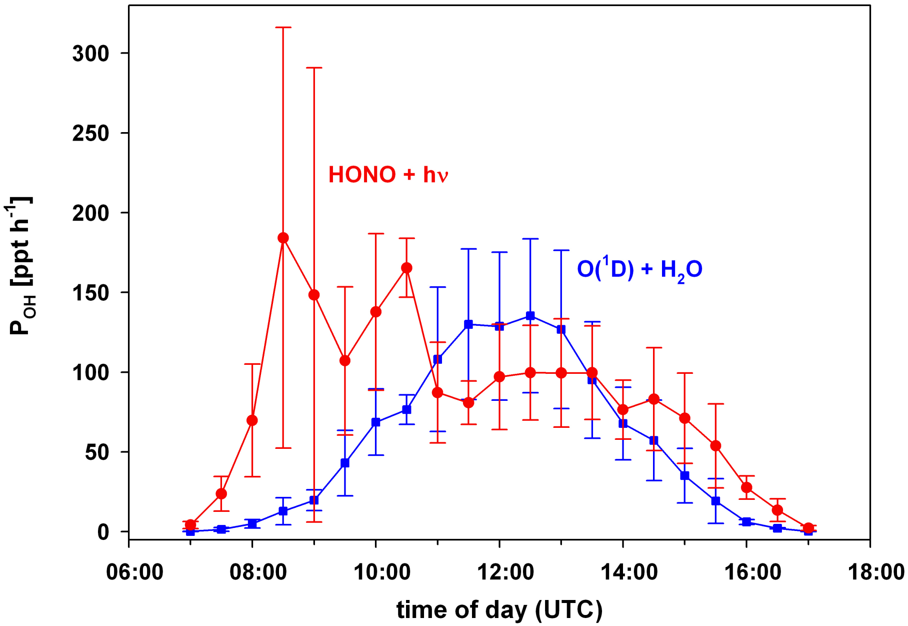

Fig. 7. Comparison for the seven clear days of the campaign of calculated primary OH production by HONO and ozone photolysis (means and standard deviations).